Structural Engineering and Mechanics, *Vol. 53, No. 4 (2015) 781-790*
DOI: http://dx.doi.org/10.12989/sem.2015.53.4.781

Bending analysis of a single leaf flexure using higher-order beam theory

Nghia Huu Nguyen and Dong-Yeon Lee*

School of Mechanical Engineering, Yeungnam University, Gyeongsan 712-749, Republic of Korea

(Received October 29, 2014, Revised January 4, 2015, Accepted January 7, 2015)

Abstract. We apply higher-order beam theory to analyze the deflections and stresses of a cantilevered single leaf flexure in bending. Our equations include shear deformation and the warping effect in bending. The results are compared with Euler-Bernoulli and Timoshenko beam theory, and are verified by finite element analysis (FEA). The results show that the higher-order beam theory is in a good agreement with the FEA results, with errors of less than 10%. These results indicate that the analysis of the deflections and stresses of a single leaf flexure should consider the shear and warping effects in bending to ensure high precision mechanism design.

Keywords: single leaf flexure; higher-order beam theory; shear deformation; bending; stress analysis

1. Introduction

Many theories have been applied to analyze the bending of a beam with the objective of finding a more accurate solution. The Euler-Bernoulli beam theory (EBT) is a classical beam theory that neglects shear effects. Timoshenko beam theory (TBT) uses the assumption that bending deformation includes constant transverse shear deformation that is expressed by shear factor in the calculated formula (Hutchinson, 2001). Similar to the TBT, the higher-order beam theory (HBT) considers transverse shear deformation in bending that is not constant over a cross-section due to the warping effect in bending. The HBT has been applied to the bending analysis of beams (Levinson 1981, Reddy *et al*. 1997, 2001, Wang *et al*. 2000).

In precision machine design with very high accuracy requirements such as micro-electro-mechanical systems (MEMS) and nano-electro-mechanical systems (NEMS) devices that use the micro- or nanoscale, accurate analysis is a challenge for design calculations. A single leaf flexure (SLF) is frequently used in precision machines, especially in nano-scanner devices due to advantages such as easily obtainable uniform spring material and no friction characteristic, its smooth motion. Many previous studies have used the single leaf in the design of precision devices, (Schitter *et al.* 2008, Hayashi *et al.* 2012, Brouwer *et al.* 2013), or as a combined hinge and leaf spring (Yong *et al*. 2009, Kim *et al*. 2012, Lee *et al*. 2012, Bhagat *et al*. 2014).

Many studies have considered the application of beam theory to bending analysis. For example,

*Corresponding author, Professor, E-mail: dylee@ynu.ac.kr

http://www.techno-press.org/?journal=sem&subpage=8 ISSN: 1225-4568 (Print), 1598-6217 (Online)

Levinson (1981) considered the HBT applied to a cantilever beam under a concentrated load at the free end. However, the authors only considered the theoretical results of deflection, which was not verified by another method, and a stress analysis was not presented. Reddy *et al.* (1997, 2001), Wang *et al.* (2000) demonstrated the HBT and gave examples for the case of bending applied to a cantilever beam under a distributed load. The results were not compared with another analysis method, and the formulas for stresses were shown but not verified by another method. Recent research in precision machines (Koseki *et al.* 2002) gave formulas for the deflection of a prismatic beam in bending. However, the shear deformation and warping effect were not considered, and a stress analysis was not included. In Kim *et al.* (2004), the shear effect is considered but the warping effect is not mentioned. Stress was presented, but the formula for stress was not shown in detail. Shear deformation was considered in Kim *et al.* (2012), and bending stress was described. However, the warping effect and shear stress were not mentioned in their research.

In this study, we analyzed the deflection and stresses of a SLF in bending by applying the HBT. Shear deformation and shear stress were considered, and the warping effect was included in the bending analysis. The results of HBT were compared with EBT and TBT. In addition, FEA was conducted to verify the results of our theoretical analysis. The parameters of length, width, and thickness of the SLF were varied to test their sensitivity to the deflections and stresses.

2. Generalized modeling of a single leaf flexure

Our model of SLF is shown in Fig. 1. The model was used to describe the movement of a body smoothly and in nano-resolution, as discussed in (Schitter *et al.* 2008, Lee *et al.* 2012, Bhagat *et al.* 2014). The dimensions of the SLF are l, b, and t (the length, width, and thickness, respectively). When forces F_y, F_z or moments M_y, M_z are applied to the SLF, bending deformation occurs. These loads cause deflections at the free end in similar manner, and bending and shear stress also occur inside the body in similar manner. Thus, in this study, the deflection, bending, and shear stress due to loading F_z were investigated. Fig. 2 shows a schematic diagram of a compliant mechanism using a SLF. The upper, lower moving parts and the fixed base are connected with SLFs. The monolithic compliant mechanism is usually fabricated via a wire electro-discharge machining. Therefore, it is free from the friction between moving parts.

2.1 EBT

In this study, the SLF is considered as a cantilever beam with a fixed and a free ends. When the concentrated load is applied at the free end, the deflection due to bending is given by (Crandall and Dahl 1978)

$$w^E = \frac{F_z L^3}{6EI}\left[3\left(\frac{x}{L}\right)^2 - \left(\frac{x}{L}\right)^3\right] \tag{1}$$

Where E is the modulus of longitudinal elasticity (Young's modulus), I is the second inertia moment about the y-axis

The bending stress is given by

$$\sigma^E{}_{xx} = E\varepsilon^E{}_{xx} = Ez\frac{d^2w^E}{dx^2} = \frac{F_z z}{I}(x - L) \tag{2}$$

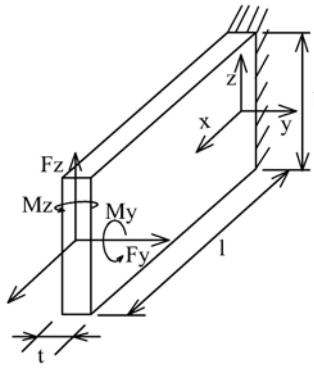

Fig. 1 Schematic diagram of single leaf flexure

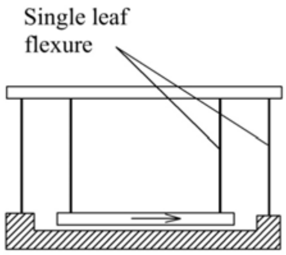

Fig. 2 Schematic diagram of compliant mechanism with single leaf flexures

The shear deformation was not considered in EBT, so the shear stress is given by

$$\tau^E{}_{xz} = G\gamma^E{}_{xz} = 0 \tag{3}$$

2.2 TBT

TBT considers a constant shear deformation over the cross section. The deflection and rotation of beam were calculated by using the summarized formulas in Table 2.2.1 (Wang *et al.* 2000), shown as

$w^T = w^E + \frac{1}{GAk_s}\left(M^E(x) - M^E(0)\right)$, where $M^E = -EI\frac{d^2w^E}{dx^2}$ is the bending moment. The deflection is obtained as

$$w^T = \frac{F_zL^3}{6EI}\left[3\left(\frac{x}{L}\right)^2 - \left(\frac{x}{L}\right)^3\right] + \frac{F_zL}{GAk_s}\left(\frac{x}{L}\right) \tag{4}$$

where $k_s = \frac{10(1+\nu)}{12+11\nu}$ is the Timoshenko shear coefficient and ν is Poisson's ratio, G is the modulus of transverse elasticity, A is the cross sectional area. The first term of the right-hand side of Eq. (4) corresponds to Eq. (1). Due to the additional shear deformation of the second term of the right-hand side of Eq. (4), the vertical deflection resulting from TBT is more than the deflection from EBT.

The rotation is given as

$$\phi^T = -\frac{dw^E}{dx} = \frac{F_z}{EI}\left(\frac{x^2}{2} - Lx\right) \tag{5}$$

The bending stress is

$$\sigma^T{}_{xx} = E\varepsilon^T{}_{xx} = Ez\frac{d\phi^T}{dx} = \frac{F_z z}{I}(x-L) \tag{6}$$

The TBT assumed that the shear deformation is constantly present in bending, thus shear stress is given by

$$\tau^T{}_{xz} = G\gamma^T{}_{xz} = G\left(\phi^T + \frac{dw^T}{dx}\right) = \frac{F_z}{Ak_s} \tag{7}$$

2.3 HBT

The HBT assumed that the shear deformation in bending is not constant over a cross-section due to the warping effect in bending. The expressions of the relationship between the HBT and EBT for general bending solution were presented (Reddy *et al.* 1997, Wang *et al.* 2000). The bending moment, shear force, slope and deflection were defined, respectively

$$M^R = M^E + C_1 x + C_2 \tag{8}$$

$$\alpha\left(\frac{F_{xx}\bar{D}_{xx}}{D_{xx}\bar{A}_{xz}} - \frac{\bar{F}_{xx}}{\bar{A}_{xz}}\right)\frac{d^2Q^H}{dx^2} - \left(\frac{\hat{A}_{xz}}{\bar{A}_{xz}}\right)Q^H + \left(\frac{\bar{D}_{xx}}{D_{xx}}\right)(Q^E + C_1) = 0 \tag{9}$$

$$D_{xx}\phi^H = -D_{xx}\frac{dw^E}{dx} + \alpha\left(\frac{F_{xx}}{\bar{A}_{xz}}\right)Q^H + C_1\frac{x^2}{2} + C_2 x + C_3 \tag{10}$$

$$D_{xx}w^H = D_{xx}w^E + \left(\frac{\bar{D}_{xx}}{\bar{A}_{xz}}\right)\left(\int Q^H(\eta)d\eta\right) - C_1\frac{x^3}{6} - C_2\frac{x^2}{2} - C_3 x - C_4 \tag{11}$$

$$Q^H = C_5 sinh\lambda x + C_6 cosh\lambda x + \frac{\mu}{\lambda^2}(Q^E + C_1) \tag{12}$$

Where $\alpha = \frac{4}{3h^2}$;$\beta = 3\alpha = \frac{4}{h^2}$; $F_{xx} = \frac{3h^2 EI}{20}$; $\bar{D}_{xx} = \frac{4EI}{5}$; $D_{xx} = EI$; $\bar{A}_{xz} = \frac{8GI}{h^2}$; $\bar{F}_{xx} = \frac{4h^2 EI}{35}$; $\hat{A}_{xz} = \frac{32GI}{5h^2}$; $I = \frac{th^3}{12}$; $\mu = \frac{420}{h^2(1+\nu)}$; $\lambda = \sqrt{\frac{420}{h^2(1+\nu)}}$

and M^E, Q^E, w^E are the bending moment, shear force, deflection based on Euler-Bernoulli beam theory, respectively and h is the depth of beam (in this study, $h = b$), and C_i (i =1, 2, 3, 4, 5, 6) are the constants of integration.

The cantilevered SLF under a concentrated load at the free end was not investigated yet by HBT in previous researches (Wang *et al.* 2000). In this study, we applied the fixed and free boundary conditions upon the cantilevered SLF to find the constants of integration that are shown as follows;

$$C_1 = C_2 = C_3 = 0, C_4 = \left(\frac{Eh^2}{10G}\right)\left(\frac{F_z}{\lambda}\right)tanh\lambda L, C_5 = F_z tanh\lambda L, C_6 = -F_z$$

Thus, from Eq. (12) the shear force is obtained

$$Q^H = F_z(tanh\lambda L sinh\lambda x - cosh\lambda x + 1) \tag{13}$$

The deflection is determined from Eq. (11)

$$w^H = \frac{F_z L^3}{6EI}\left[3\left(\frac{x}{L}\right)^2 - \left(\frac{x}{L}\right)^3\right] + \left[\frac{F_z L^3}{5EI}(1+\nu)\left(\frac{h}{L}\right)^2\right]\left(\frac{x}{L}\right) + \left[\frac{F_z L^3}{5EI}(1+\nu)\left(\frac{h}{L}\right)^2\right]\left[\frac{1}{\lambda L}(tanh\lambda L cosh\lambda x - sinh\lambda x - tanh\lambda L)\right] \quad (14)$$

The first, second and third term of the right-hand side of Eq. (14) correspond to the EBT, TBT and HBT contributions, respectively.

The slope is obtained from Eq. (10)

$$\phi^H = \frac{F_z}{EI}\left(\frac{x^2}{2} - Lx\right) + \left(\frac{F_z h^2}{40GI}\right)(tanh\lambda L sinh\lambda x - cosh\lambda x + 1) \quad (15)$$

From Eqs. (14) and (15), the bending and shear stresses are obtained.

Bending stress $\sigma^H{}_{xx} = E\varepsilon^H{}_{xx} = E\left[z\frac{d\phi^H}{dx} - \alpha z^3\left(\frac{d\phi^H}{dx} + \frac{d^2 w^H}{dx^2}\right)\right]$ is as follows;

$$\sigma^H{}_{xx} = E\left[\left(\frac{F_z z}{EI}(x-L) + \left(\frac{F_z z\lambda h^2}{40GI} - \frac{F_z z^3\lambda}{30GI} - \frac{2F_z z^3\lambda}{15GI}\right)(tanh\lambda L cosh\lambda x - sinh\lambda x)\right)\right] \quad (16)$$

The shear stress is defined as $\tau^H{}_{xz} = G\gamma^H{}_{xz} = G\left[\phi^H + \frac{dw^H}{dx} - \beta z^2\left(\phi^H + \frac{dw^H}{dx}\right)\right]$, thus the final shear stress is obtained as follows;

$$\tau^H{}_{xz} = G\left(1 - \frac{4z^2}{h^2}\right)\left(\frac{F_z h^2}{8GI}\right)(tanh\lambda L sinh\lambda x - cosh\lambda x + 1) \quad (17)$$

3. FEA verification

ANSYS 14.0 FEA commercial FEA software (PA 15317, USA) was used to verify the results of theory. The default dimensions of the SLF parameters are l=10 mm, b=4 mm, and t=0.5 mm. To test the applicability of the theoretical equations, the sensitive parameters were varied as follows: length l=5 to 20 mm, width b=2 to 8 mm, and thickness t=0.25 to 1 mm. The material used in the FEA simulation is aluminum 6061, with a loading of F_z=1 N. The goal of our research is to analyze and calculate the deflection and stresses of a SLF in bending by EBT, TBT, and HBT, and compare these results with the simulated results from FEA.

Tables 1 and 2 show the calculated results of the deflection, bending stress, and shear stress using the three beam theories and the comparison with results of FEA at the default values. Table 1 shows that the HBT has the lowest error of only 1.10%, the EBT has an error of 9.90%, and TBT is closest to the HBT at 1.13%. The error of the HBT is also the lowest for shear stress, 0.29%. This result is very far from the result of TBT, which is 21.76%, as shown in Table 2. However, the HBT bending stress result gives the highest error at 4.99%, while the EBT and TBT are only 0.99%. These results indicate that the HBT can be chosen for design; however, to ensure the reliability of the calculations, the sensitive parameters need to be analyzed.

Figs. 3-5 show the simulation results for the deflection sensitivity of the SLF with variations of length, thickness, and width. They show that the parabolic curves of the variation of deflection δ_z are similar to those from FEA. The figures also show the curves of the errors of the three beam theories with the FEA results. We note that Error 3 of HBT is the lowest, and the errors of EBT are

Table 1 Comparison of deflection between theory and FEA results at the default values of flexure

Method/theory	Deflection δ_z (mm)	FEA/theory error (%)
FEA	0.0020135	-
EBT	0.0018142	9.9
TBT	0.0020363	-1.13
HBT	0.0020356	-1.10

Table 2 Comparison of bending and shear stress between theory and FEA results at the default values of flexure

Method/theory	Shear stress τ_{xz} (N/mm^2)	FEA/theory error (%)	Bending stress σ_{xx} (N/mm^2)	FEA/theory error (%)
FEA	0.752160	-	7.055100	-
EBT	0.000000	-	7.125000	-0.99
TBT	0.588462	21.76	7.125000	-0.99
HBT	0.750000	0.29	7.372074	-4.99

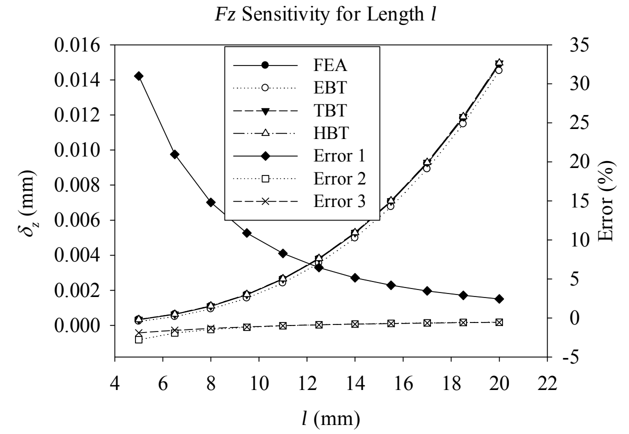

Fig. 3 Variation of δ_z according to length l under loading F_z ((Error 1= [FEA- (EBT)]×100/ FEA; Error 2= [FEA- (EBT+TBT)] ×100/ FEA; Error 3= [FEA- (EBT+TBT+HBT)] ×100/ FEA))

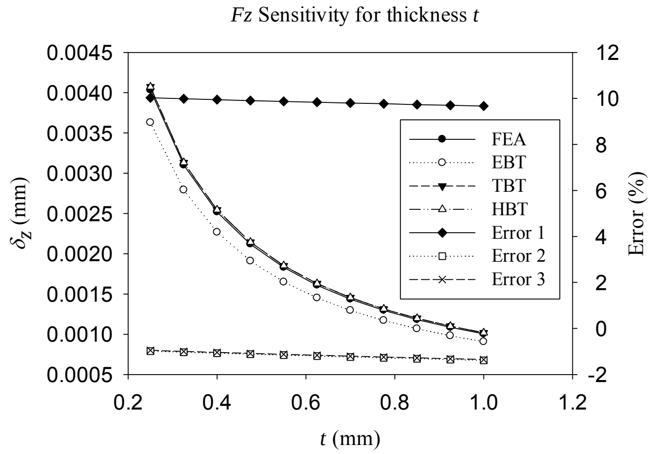

Fig. 4 Variation of δ_z according to thickness t under loading F_z

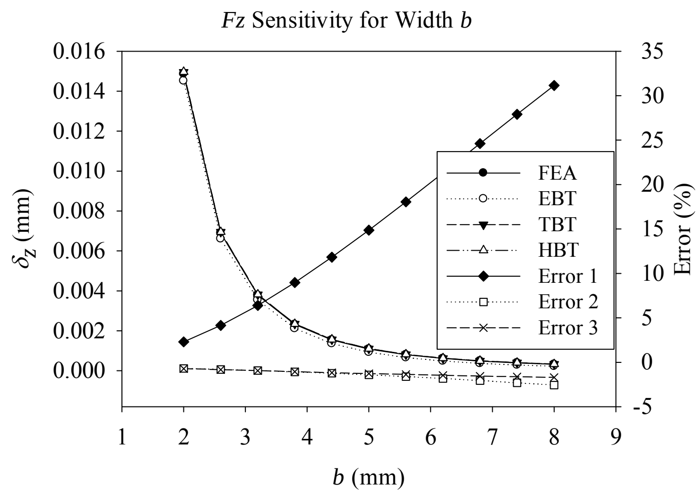

Fig. 5 Variation of δ_z according to width *b* under loading F_z

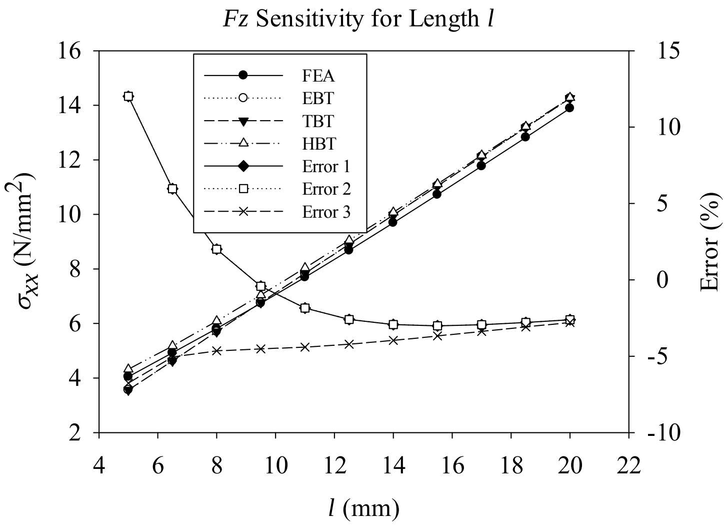

Fig. 6 Variation of σ_{xx} according to length *l* under loading F_z

significantly higher by up to 30%. Although the errors of HBT and TBT are quite close to each other at the default values, the HBT is still lower 2% while the TBT is up to 3%. Figures 6-8 show the sensitivity results of bending stress according to variations of length, thickness, and width. The errors of HBT are also lower, while the EBT and TBT errors are up to 12%.

Similar to the preceding analysis, Figs. 9-11 show the results of the sensitivity simulation of shear stress with variations of length, thickness, and width. Because the shear stress is not considered in the EBT, only the curves of TBT and HBT are shown and compared with FEA. There is a significant difference in the errors between TBT and HBT: the TBT error is up to 27%, the HBT error is a maximum of 7.31%.

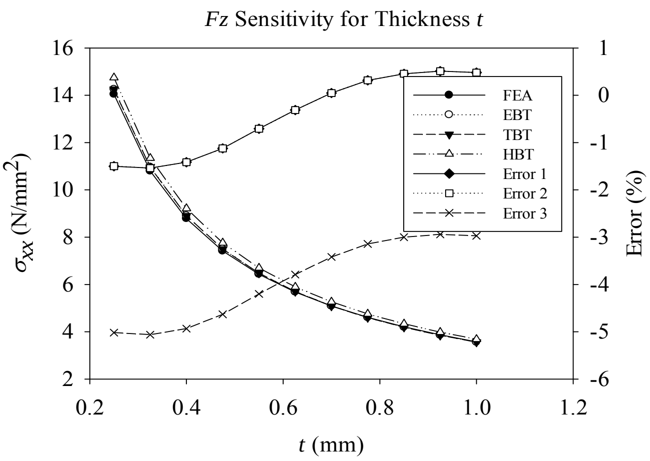

Fig. 7 Variation of σ_{xx} according to thickness t under loading F_z

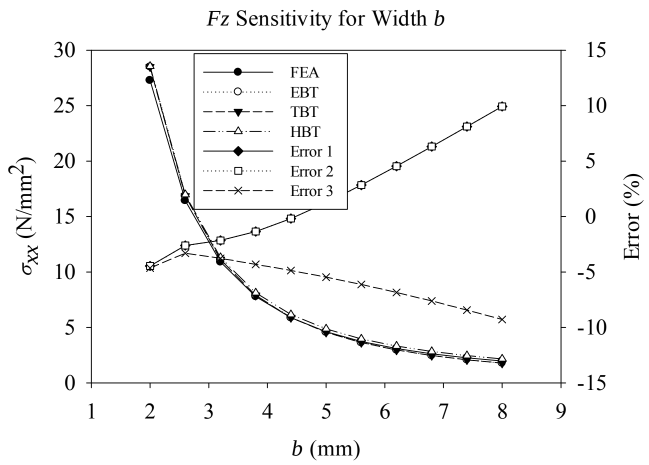

Fig. 8 Variation of σ_{xx} according to width b under loading F_z

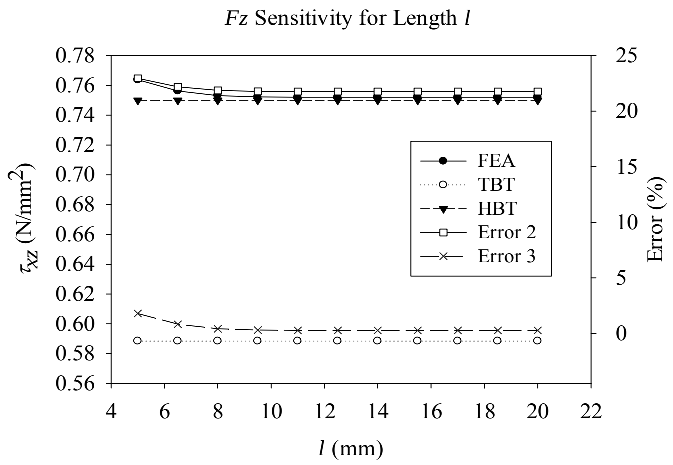

Fig. 9 Variation of τ_{xz} according to length l under loading F_z

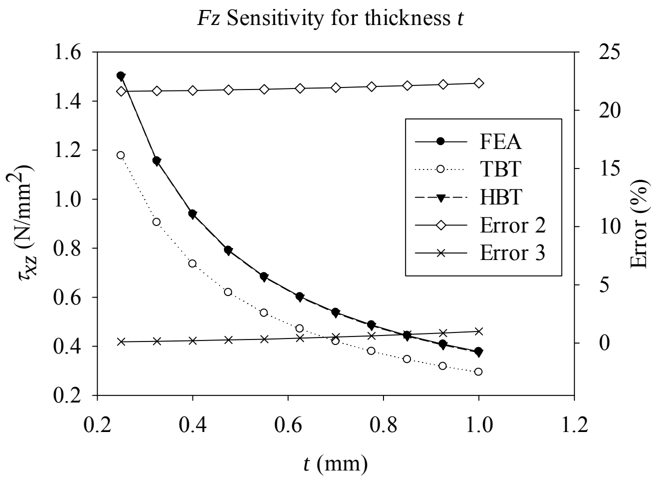

Fig. 10 Variation of τ_{xz} according to thickness t under loading F_z

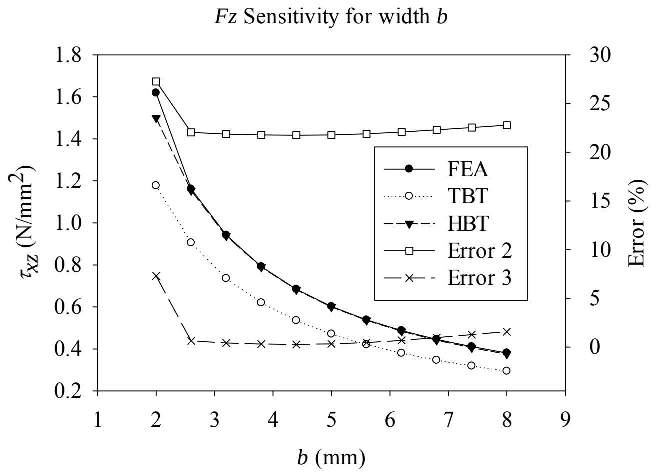

Fig. 11 Variation of τ_{xz} according to width b under loading F_z

4. Conclusions

In this study, the deflections, rotations and stresses of a cantilevered SLF in bending were analyzed by using the HBT, TBT, and EBT. All the results were verified via FEA at both the default and variation values. The analysis results show that the HBT, which includes shear deformation and the warping effect in bending, were the closest to those of FEA (all the errors are lower than 10%). The deflection and rotation angle of HBT include the results from EBT and TBT. Because the complete deflection and stress analysis of the cantilevered SLF has been performed with sufficient accuracy, the present work suggests that the HBT should be applied to the design of a SLF in bending that includes the shear and warping effects. Moreover, the complete compliance matrix for the SLF could be derived by using the present bending analysis.

Acknowledgments

This research was supported in part by Basic Science Research Program through the National Research Foundation of Korea (NRF) funded by the Ministry of Science, ICT and Future Planning (NRF-2012R1A1A2004056). This research was also supported in part by Basic Science Research Program through the National Research Foundation of Korea (NRF) funded by the Ministry of Education (NRF-2013R1A1A4A01009657).

References

Bhagat, U., Shirinzadeh, B., Clark, L., Chea, P., Qin, Y., Tian, Y. and Zhang, D. (2014), "Design and analysis of a novel flexure-based 3-DOF mechanism", *Mech. Mach. Theo*., **74**, 173-187.

Brouwer, D.M., Meijaard, J.P. and Jonker, J.B. (2013), "Large deflection stiffness analysis of parallel prismatic leaf-spring flexures", *J. Precis. Eng*., **37**, 505-521.

Crandall, S.H. and Dahl, N.C. (1978), *Introduction to the Mechanics of Solids*, McGraw-Hill, New York, USA.

Hayashi, M. and Fukuda, M. (2012), "Generation of nanometer displacement using reduction mechanism consisting of torsional leaf spring hinges", *Int. J. Precis. Eng. Man*., **13**(5), 679-684.

Hutchinson, J.R. (2001), "Shear coefficients for Timoshenko beam theory", *J. Appl. Mech.-T.*, ASME, **68**(1), 87-92.

Kim, J.H., Kim, S.H. and Kwak, Y.K. (2004), "Development and optimization of 3-D bridge-type hinge mechanisms", *Sens. Actuat.,* **116**, 530-538.

Kim, J.J., Choi., Y.M., Ahn, D., Hwang, B., Gweon, D.G. and Jeong, J. (2012), "A millimeter-range flexure-based nano-positioning stage using a self-guided displacement amplification mechanism", *Mech. Mach. Theo*., **50**, 109-120.

Koseki, Y.T.A. and Koyachim N. (2002), "Kinematic analysis of translational 3-Dof micro parallel mechanism using matrix method", *Adv. Robot*., **16**(3), 251-264.

Lee, M.Y., Park, E.J., Yeom, J.K., Hong, D.P. and Lee, D.Y. (2012), "Pure nano-rotation scanner", *Adv. Mech. Eng*., Article ID 962439, 1-11.

Levinson, M. (1981), " A New Rectangular Beam Theory", *J. Sound. Vib*., **74**(1), 81-87.

Reddy J.N., Wang, C.M. and Lee, K.H. (1997), "Relationships between bending solutions of classical and shear deformation beam theories", *Int. J. Solid. Struct*., **34**(26), 3373-3384.

Reddy, J.N., Wang, C.M., Lim, G.T. and Ng, K.H. (2001), "Bending Solutions of Levinson Beams and Plates in Terms of the Classical Theories", *Int. J. Solid. Struct*., **38**, 4701-4720.

Schitter, G., Thurner, P.J. and Hansma, P.K. (2008), "Design and input-shaping control of a novel scanner for high-speed atomic force microscopy", *Mechatronics*, **18**, 282-288.

Wang, C.M., Reddy, J.N. and Lee, K.H. (2000), *Shear Deformable Beams and Plates: Relationships with Classical Solutions, Bending of beams,* Elsevier Science, UK.

Yong, Y.K., Aphale, S.S. and Moheimani, S.O.R. (2009), "Design, identification, and control of a flexure-based XY stage for fast nanoscale positioning", *IEEE T. Nanotech*., **8**(1), 46-54.

CC